In **Advances in Renewable Energies Offshore: Proceedings of the 3rd International Conference on Renewable Energies Offshore (RENEW 2018), October 8-10, 2018, Lisbon, Portugal. 1st Edition. pp 23-30**
2019
Ed Carlos Guedes Soares
ISBN 9781138585355
https://archimer.ifremer.fr/doc/00461/57308/

How to correctly measure turbulent upstream flow for marine current turbine performances evaluation?

Gaurier Benoit[1], Germain Gregory[1], Pinon G[2]

[1] IFREMER
[2] UNIV LE HAVRE NORMANDIE

Abstract :

Until now, no pan-European nor worldwide consensus on appropriate test methodologies and practices have yet been implemented in order to carry out standard laboratory tests. For performance test (in laboratory as well as in-situ), the measurement of the upstream flow velocity is required to calculate kinetic energy, especially when the turbulence intensity is high. These flow fluctuations affect significantly the performance and fatigue behaviour of tidal turbines. However, for a good accuracy the upstream flow measurement needs to be performed in a synchronous way with the turbine parameters. In this paper, we study the time and space correlation between velocity measurements and turbine parameters in order to evaluate and improve the specifications given in IEC TS 62600–200 to 202 for the current profiler placement relative to the turbine.

ABSTRACT: Until now, no pan-European nor worldwide consensus on appropriate test methodologies and practices have yet been implemented in order to carry out standard laboratory tests. For performance test (in laboratory as well as *in-situ*), the measurement of the upstream flow velocity is required to calculate kinetic energy, especially when the turbulence intensity is high. These flow fluctuations affect significantly the performance and fatigue behaviour of tidal turbines. However, for a good accuracy the upstream flow measurement needs to be performed in a synchronous way with the turbine parameters. In this paper, we study the time and space correlation between velocity measurements and turbine parameters in order to evaluate and improve the specifications given in IEC TS 62600-200 to 202 for the current profiler placement relative to the turbine.

1 INTRODUCTION

Tank testing is primarily undertaken to establish the behaviour of a tidal energy converter at model scale and to identify the impact of different test configurations (flow and prototype characteristics) on device performance. At present there is no pan-European or worldwide consensus on appropriate test methodologies and practices to be implemented, even if procedures developed within the EC EquiMar (Ingram et al. 2011) and MaRINET (Gaurier et al. 2015) projects, have been carried out. Today, international best practice guidelines for tidal turbine testing are under development by the International Electrotechnical Commission (IEC) (Day et al. 2014). For performance test (in laboratory as well as *in-situ*), the measurement of the upstream flow velocity is required to calculate kinetic energy, especially when the turbulence intensity is high (McNaughton et al. 2015), (Durán Medina et al. 2017). Indeed, it has been shown that most of the tidal energy sites have a high level of tubulence (Thomson et al. 2012). These flow fluctuations affect significantly the performance and fatigue behaviour of tidal turbines. However, for a good accuracy the upstream flow measurement needs to be performed in a synchronous way with the turbine parameters.

After the presentation of the experimental set-up, we propose, in this paper, to study the time and space correlation between velocity measurements and turbine parameters, in order to evaluate and improve (if necessary) the specifications given in IEC TS 62600-200 to 202 (Marine Energy 2013), (Marine Energy 2015), (Marine Energy 2019) for the current profiler placement relative to the turbine (Germain et al. 2017), (Germain et al. 2018).

2 EXPERIMENTAL SET-UP

2.1 *The wave and current flume tank*

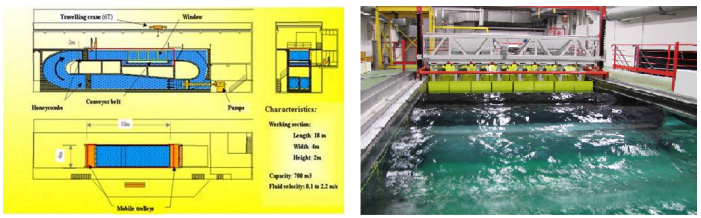

Figure 1: The wave and current flume tank of Ifremer

The tests presented in this paper have been carried out in the wave and current flume tank of Ifremer at Boulogne-sur-mer, France (figure 1). The dimensions of the testing area of the tank are $18m$ long, $4m$ wide and $2m$ deep. By means of porous grid and honeycomb placed at the inlet of the working section, a tur-

bulent intensity of $I_\infty = 1.5\%$ can be achieved. Without these straightener devices, the turbulence in the tank can reach $I_\infty \simeq 15\%$, accessing to the fully developed turbulence generated by the two pumps of the tank, which is close to the *in-situ* measured values (Thomson et al. 2012).

2.2 *The velocity measurement facilities*

Two different velocimeters are usually used in the tank for measuring the flow parameters. The first one is based on laser beams: the Laser Doppler Velocimeter (LDV). This technique is a non-intrusive principle, which allows the measurement of velocity at a point in a flow field with a high temporal resolution. Whenever a reflecting particle entrained in the fluid passes through the intersection of two laser beams, the scattered light received from the particle fluctuates in intensity, see figure 2 from (Dantec Dynamics 2018). LDV makes use of the fact that the frequency of this fluctuation is equivalent to the Doppler shift between the incident and scattered light, and is thus proportional to the component of particle velocity. The LDV system available at Ifremer is 2 dimensional, *i.e.* composed of 4 laser beams with 2 different wave lengths (blue and green).

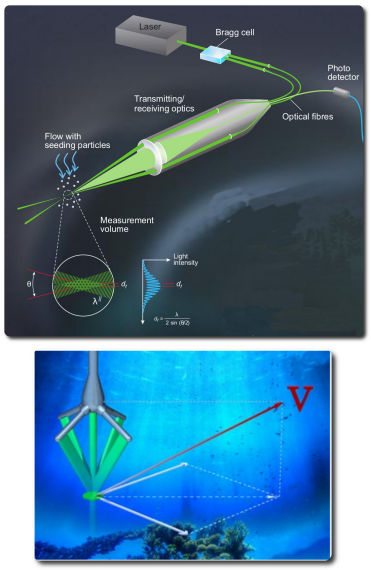

Figure 2: The LDV (left) and ADV (right) probes and their measurement volumes

The measurement volume is $2.51mm$ long by the laser beams thickness of $0.12mm$, which results of $V_{LDV} \simeq 0.01mm^3$. The distance between the probe and the measurement point is $530mm$ into the water. The water of the tank is seeded with particles which should be small enough to follow the flow, yet large enough to scatter sufficient light to obtain a good signal-to-noise ratio. Typically the size of particles used in the Ifremer flume tank is $10\mu m$. These particles are spherical and composed of silver coated glass. For the acquisition signal, the data rate depends on the number of particles detected by the system. Usually, the averaged data rate is between $100Hz$ and $1000Hz$ depending on the conditions. However, the sampling frequency is irregular due to the fact that one measurement value corresponds to one detected particle in the volume.

The second velocity measurement facility is an Acoustic Doppler Velocimeter (ADV). This system works by sending out a short acoustic pulse from the transmit element. When the pulse travels through the focus point for the receiver beams, the echo is recorded in each of the acoustic receiver elements, see figure 2, from (Nortek USA 2018). The echo is then processed to find the Doppler shift. The velocity vector is recorded in 3D.

The sampling volume is located $50mm$ from the transmitter to provide undisturbed measurements. The chosen size of this volume is a cylinder with $9mm$ high and $5mm$ diameter, so $V_{ADV} \simeq 200mm^3$. The seeding material is the same than the one used for the LDV. On the contrary to the LDV, the sampling frequency of the ADV signal is regular. This frequency can be set between $10Hz$ and $200Hz$, but the signal quality strongly depends on the particle number into the water.

2.3 *The turbine model*

The 1/20th scale turbine model (see picture 3) used for this study is very similar to the ones used in (Mycek et al. 2014). More particularly, blades are exactly the same than in (Gaurier et al. 2015). The hub diameter however is slightly larger. So, the diameter of the disc described by the blades of this new turbine is now $D = 724mm$ (radius $R = 362mm$), instead of $700mm$ in previous studies. However, the machine performances are the same, as shown by (Gaurier et al. 2017).

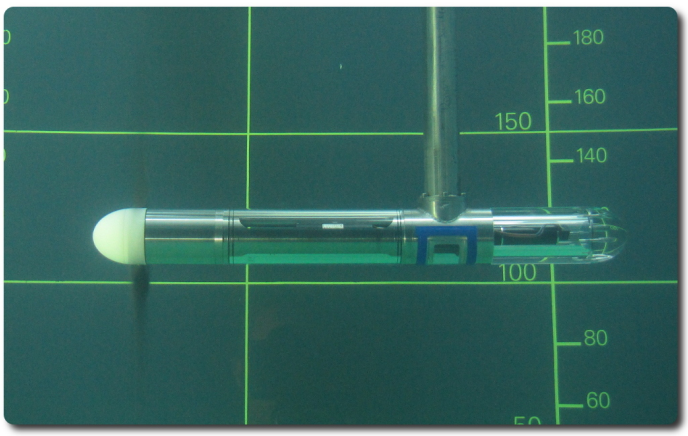

Figure 3: The 3-bladed instrumented turbine in the wave and current flume tank of Ifremer

This hub diameter size change is due to the fact that a complete new instrumentation equipment takes place inside the hub. This new experimental equipment has been designed based on the one developed in (Payne et al. 2017). Each blade root is now equipped with a specific load-cell including 5 different channels: 2 forces and 3 moments.

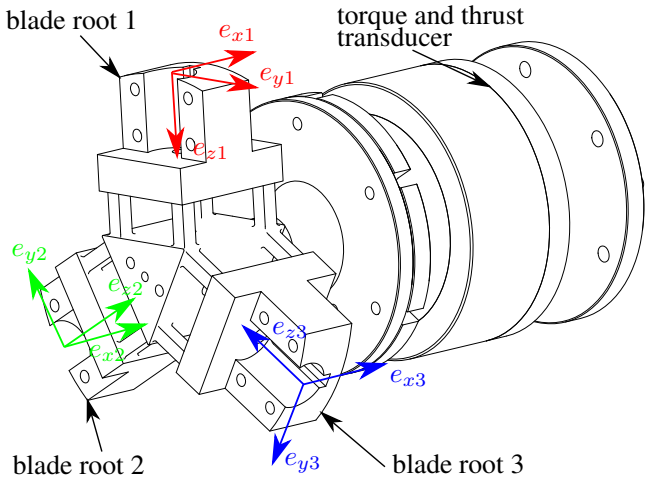

Figure 4: The blade root load-cell with its three coordinate systems and the torque and thrust transducer

In addition to this new multi-components blade root load-cell, the torque and the thrust applied on the main rotation axis are now measured. This waterproof transducer is positioned upstream of the seals of the machine to prevent measuring the friction effects (figure 4). The blade root load-cell and the torque and thrust transducer are custom made by the French company Sixaxes (Sixaxes 2017) in partnership with Ifremer. The 48 shielded cables coming from these transducers are routed through a 52 channels slipring enabling the rotation. These low voltage signals are amplified by an electronic signal processing unit, located outside of the turbine and of the water as well. The motor shaft is connected to the turbine shaft through a motor-gearbox enabling suitable torque and rotation speed ratings.

The turbine is controlled to maintain a constant rotational speed ω. In the following, the turbine power $P = Q\omega$, with Q the rotor torque, is presented as a non-dimensional coefficient C_P and usually plotted versus the Tip-Speed-Ratio (TSR), both expressed with the classical formula 1.

$$C_P = \frac{Q\omega}{\frac{1}{2}\rho S U_\infty^3} \quad \text{and} \quad TSR = \frac{R\omega}{U_\infty} \tag{1}$$

where ρ is the water density, S is the rotor area and U_∞ is the ambient velocity.

3 EFFECT OF THE UPSTREAM VELOCITY MEASUREMENT ON TURBINE PERFORMANCES

For model scale studies in laboratory, an accurate measurement of this ambient velocity is required to properly evaluate the turbine performance. This is especially necessary when the velocity fluctuations are high, because of the turbulence generated by bathymetry variations or because of surface waves. However, this measurement can be performed in two different ways:

1. from a flow calibration carried out before the turbine characterization or
2. by a simultaneous and synchronous upstream flow measurement.

In the second case, the velocity measurement has to be non-intrusive to prevent to affect the turbine parameters.

Some experimental tests have been carried out with the previously described turbine, in the flume tank of Ifremer. Two different flow velocities have been tested $U_\infty = [1.0; 1.2]m/s$ with a high turbulence intensity $I_\infty \simeq 15\%$, *i.e.* without the flow straightener. An initial velocity measurement has been performed with the LDV during $30min$ for the same flow conditions, at the centre of the tank section, the same location than the turbine. Table 1 summarizes the flow characterization obtained from these measurements. As explained in the previous section, LDV is 2-dimensional in the Ifremer laboratory. However, in this table, only u_L is given and stands for the in-line component of the flow. The subscript $_L$ means the long time acquisition. The classical decomposition is used here: $u_L(t) = \overline{u_L} + u'_L(t)$ with $\overline{u_L}$ the time-averaged part and $u'_L(t)$ the fluctuating part of the velocity. In addition, the two-dimensional turbulence intensity I_{2D} is given as well, using formula 2.

$$I_{2D} = 100\sqrt{\frac{\frac{1}{2}(\overline{u'^2_L} + \overline{v'^2_L})}{\overline{u_L}^2 + \overline{v_L}^2}} \tag{2}$$

Table 1: Flow characterization obtained from a one point LDV measurements during $30min$ with high turbulence intensity (σ stands for the standard-deviation)

	$U_\infty = 1.0m/s$	$U_\infty = 1.2m/s$
$\overline{u_L}$ $[m/s]$	0.975	1.166
$\sigma(u_L)$ $[m/s]$	0.128	0.158
I_{2D} $[\%]$	13.89	14.28

The turbine parameters have been recorded for 13 TSR in these two flow conditions. During these tests, the LDV probe was into the water as well, located $2D$ upstream of the turbine. The flow measurement was synchronous with the turbine parameter acquisition. The acquisition time was $6min$ for each TSR, which is enough for enabling the convergence. In order to process the power coefficient C_P, the velocity U_∞ can be taken from the previous long measurements from table 1: $u_L(t)$ or from the synchronously acquired measurements: $u_S(t)$. Figures 5 and 6 show the two different C_P curves processed with these two different ways. For $U_\infty = 1.0m/s$, the difference is clear between the two cases: for $TSR \geq 4$, $C_P(u_L) < C_P(u_S)$. On the contrary, for $U_\infty = 1.2m/s$ no significant differences are noticeable and $C_P(u_L) \simeq C_P(u_S)$ In order to explain the differences obtained for the case $U_\infty = 1.0m/s$ between the curves, the difference ε_u between u_L and u_S and ε_{C_P} between $C_P(u_L)$ and $C_P(u_S)$ are processed using formula 3. The results

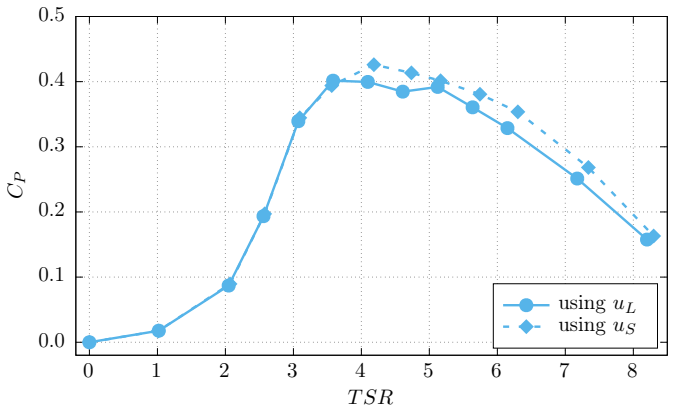

Figure 5: C_P comparison for $U_\infty = 1.0m/s$, non-dimensionalized with u_L or with u_S

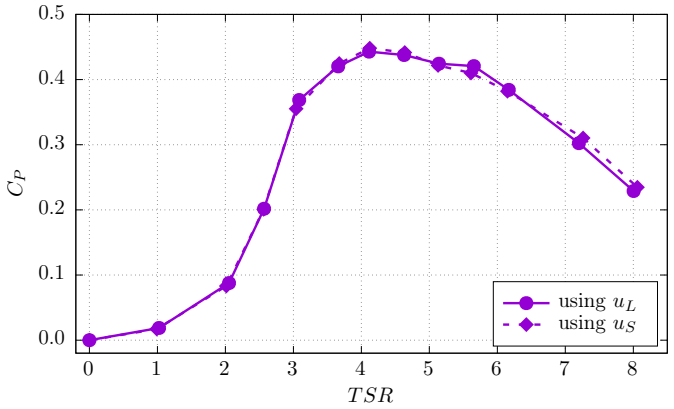

Figure 6: C_P comparison for $U_\infty = 1.2m/s$, non-dimensionalized with u_L or with u_S

obtained for all the tested TSR are shown on table 2.

$$\varepsilon_u = 100\,\frac{\overline{u_S} - \overline{u_L}}{\overline{u_L}} \quad \text{and} \quad \varepsilon_{C_P} = 100\,\frac{\overline{C_P(u_S)} - \overline{C_P(u_L)}}{\overline{C_P(u_L)}} \tag{3}$$

In this table, ε_u can reach values higher than 1%. These values are displayed in red. For these values, such a difference affects significantly the C_P curve, as shown on figure 5 for $U_\infty = 1.0m/s$: when $TSR \geq 4$, $|\varepsilon_u| \geq 2\%$ and $|\varepsilon_{C_P}| \geq 6\%$. These quite high values for ε_u are confirmed by a $6min$ sliding average process on the $30min$ long velocity acquisition: the maximum difference is then $\simeq 3\%$. That means that even if a long measurement have been done previously in order to characterize the flow, the use of a synchronous velocity measurement upstream of the turbine is required to increase the accuracy of the performance coefficients, particularly when the turbulence intensity is high, as shown in these cases. Another solution would have been to extend the acquisition time to reduce the average difference ε, but in that case, it would require a very long time to perform a 13 points TSR curve.

In addition, when a velocity acquisition is performed at the same time and synchronously with the turbine parameters, the coherence function between them can be processed as well. For the LDV measurement, this requires a re-interpolation of the signal before processing the Fourier Transform. For example, the coherence function between the turbine torque Q and

Table 2: Flow velocity obtained from the synchronous LDV measurements u_S and comparison with u_L

	$U_\infty = 1.0m/s$			$U_\infty = 1.2m/s$		
TSR	$\overline{u_S}$ $[m/s]$	ε_u [%]	ε_{C_P} [%]	$\overline{u_S}$ $[m/s]$	ε_u [%]	ε_{C_P} [%]
0.0	0.970	-0.5	+2.0	1.211	+3.8	-10.3
1.0	0.980	+0.5	-1.8	1.206	+3.4	-8.7
2.0	0.965	-1.0	+2.8	1.189	+1.9	-5.2
2.5	0.968	-0.7	+1.9	1.170	+0.3	-0.4
3.0	0.969	-0.7	+1.5	1.183	+1.4	-3.6
3.5	0.981	+0.6	-1.9	1.161	-0.4	+1.0
4.0	0.954	-2.1	+6.6	1.164	-0.2	+1.2
4.5	0.949	-2.7	+7.5	1.164	-0.2	+0.9
5.0	0.967	-0.8	+2.4	1.169	+0.2	-0.6
5.5	0.957	-1.9	+5.6	1.175	+0.8	-2.5
6.0	0.951	-2.4	+7.6	1.170	+0.3	-0.5
7.0	0.953	-2.2	+6.8	1.156	-0.9	+2.7
8.0	0.964	-1.2	+3.5	1.159	-0.7	+2.5

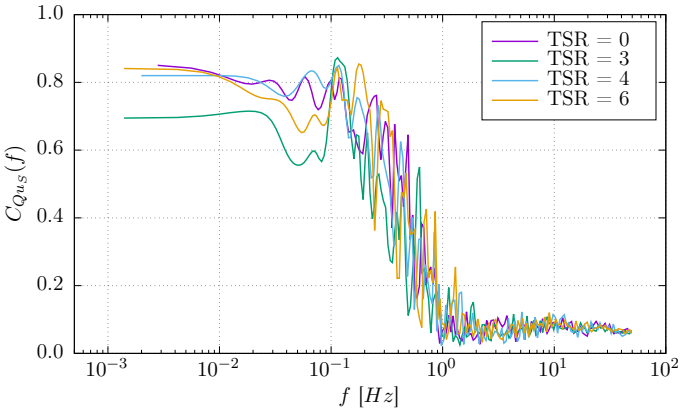

Figure 7: Coherence function between the turbine torque Q and u_S for the case $U_\infty = 1.0m/s$

u_S is displayed on figure 7 for 4 different TSR. It is interesting to notice that the tip-speed-ratio does not seem to affect the result, excepted at $TSR = 3$ for the lowest frequencies. These results confirm what has been previously observed by (Durán Medina et al. 2017) with a $4D$ distance between turbine and LDV: from frequency higher than $1Hz$, no more correlation is noticed. The authors supposed the turbine acts as a low-pass filter.

Here, the distance between the velocity measurement point and the turbine is $2D$. This distance has to be adjusted properly: not too close in order to prevent disturbing the turbine and not too far to capture the flow fluctuations perceived by the turbine. In addition, this distance may be a cause of uncertainty as well. We propose here to extend this analysis with varying distances between two different velocity measurement devices.

4 ADV-LDV COMPARISONS WITH VARYING INTER-DISTANCES

A comparison has been carried out between the two different velocimeters presented in section 2, in the tank. In that case, the flow is slightly turbulent with a turbulence level close to $I_\infty = 5\%$ and the average flow velocity is about $U_\infty = 0.8m/s$. The acquisi-

tion of the two velocimeters is simultaneous and synchronous, through an external trigger. For the ADV, a sampling frequency of $100Hz$ is chosen and the acquisition time is fixed at $10min$ for both devices. The distance d between the velocimeters has been chosen between 0 and $2m$.

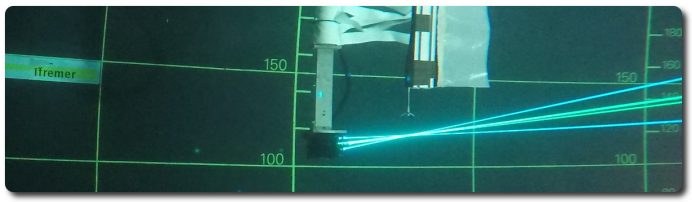

Figure 8: ADV and LDV measurement at the same point ($d = 0$)

4.1 *Velocity measurement at the same point*

For the first test, the velocimeters are positioned in order to measure at the same point, *i.e.* at the very centre of the tank section (figure 8), although their measurement volumes are different (see section 2).

Figure 9 shows a time extract of the recorded signals, for u and w components of the velocity. On this figure, it is easy to notice that the largest fluctuations of the velocity are seen at the same time and in the same way by the two velocimeters. However, the noise seems to be greater for the ADV, especially for the u component. In addition, some slight average differences appear between them: LDV shows larger values for u and lower ones for w comparing to ADV. These differences could come from a slight misalignment between the probes.

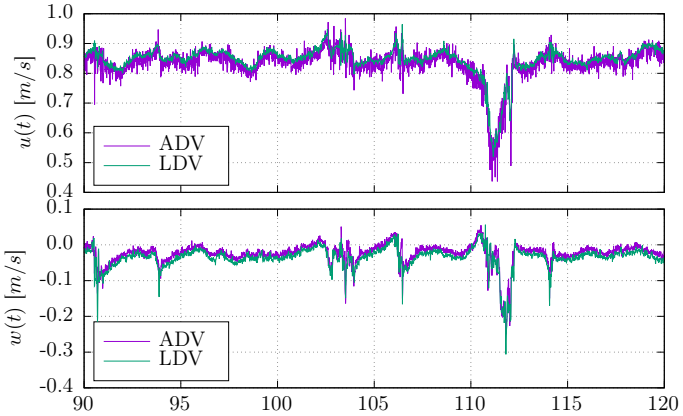

Figure 9: Temporal extract of the raw velocity measurements for $u(t)$ and $w(t)$ components for ADV and LDV

The cross-correlation ρ of these two signals (figure 10) shows a really good agreement, when the time-lag $\tau = 0s$. The value obtained at this point is higher than 0.8 for u and higher than 0.9 for w. This confirms that the fluctuating part of the signals is very close to each other.

The Power Spectral Density S_{uu} and S_{ww} of these two signals is depicted on figure 11 for u (top) and w (bottom) components of the velocity respectively. Once

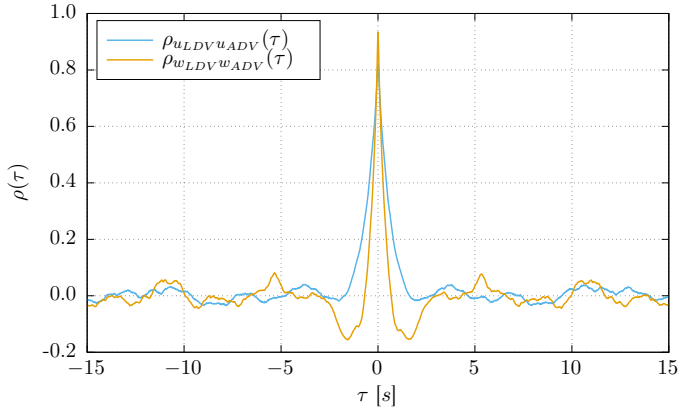

Figure 10: Cross-correlation coefficient between u_{LDV} and u_{ADV} (blue) and w_{LDV} and w_{ADV} (orange), versus the time-lag τ

again, a good agreement is observed between the velocimeters, excepted for the highest frequencies. For the ADV, S_{uu} shows an inflection point close to $3Hz$ before to remains stable for the highest frequencies. That means that from $10Hz$ the signal is mainly composed of noise, at a quite high level of energy. It is quite similar for S_{ww}, but for higher frequencies ($\simeq 30Hz$) and for lower level of energy. This confirms what has been observed on figure 9, where the noise looks higher on the u component of the ADV. On the contrary, the LDV signal follows the classical -5/3 power low slope, synonym of the Richardson-Kolmogorov energy cascade, for the full frequency range.

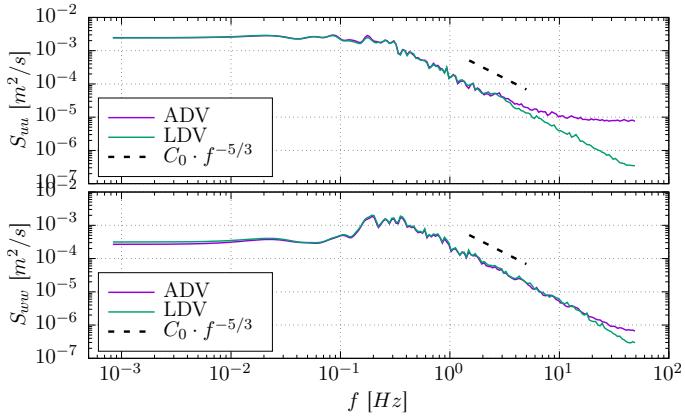

Figure 11: PSD for $u(t)$ and $w(t)$ versus the frequency, for ADV (violet) and LDV (green)

Finally, the coherence function is displayed on figure 12. As expected, the coherence is higher and stays high for a larger frequency range for u than for w. If we consider that the coherence is valid when $C(f) > 0.6$, then u_{LDV} and u_{ADV} are in good agreement for $f < 3Hz$ and w_{LDV} and w_{ADV} are coherent for $f < 6Hz$. The relatively low frequencies until which the coherence stays valid can be explained by the level of high-frequency noise in the ADV signal and also by the difference of the measurement volumes between the velocimeters (see section 2). The LDV has a very small measurement volume comparing to the ADV. This difference enables the detection

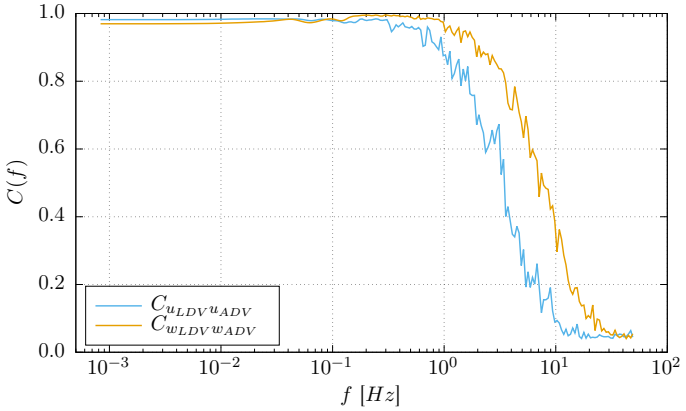

Figure 12: Coherence functions $C_{u_{LDV}u_{ADV}}$ and $C_{w_{LDV}w_{ADV}}$ versus the frequency

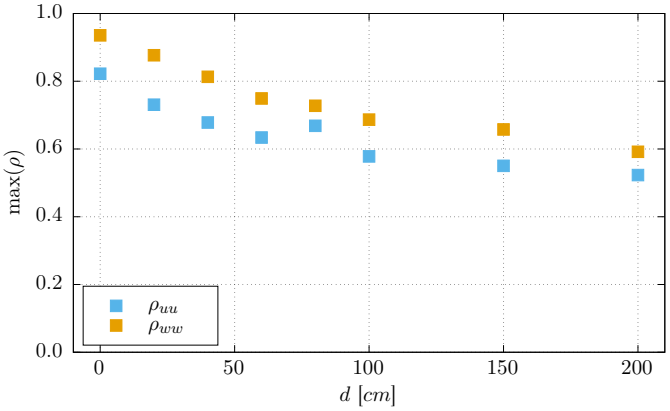

Figure 13: Maximum values of the cross-correlation ρ versus the distance d between the velocimeters

of the smallest size vortices, which contain the highest frequency velocity fluctuations. For the ADV, because of the relatively large size of the measurement volume, the smaller vortices are averaged into the high-frequency noise of the signal.

It should be very similar between the LDV and the turbine for the synchronous measurements presented in the previous section. The size of the turbine comparing to the measurement volume of the LDV acts as a low-pass filter and only the largest vortices are seen by the turbine. That can explain why the coherence function between the turbine torque and the upstream velocity is only valid when the frequency is lower that $\simeq 0.5Hz$ (figure 7). For example, when the flow velocity is $U_\infty = 1.0m/s$, $f = 0.5Hz$ means vortices size of about $0.5m$ which is lower than the turbine diameter ($0.7m$).

However, the size of the measurement volume is not the only cause of low coherence for the highest frequencies. The distance between the two velocimeters can also affect the results. In the following subsection, we extend this study with different spacing between the probes.

4.2 *Velocity measurement with* $d > 0$

In order to study the effect of the distance between the probes, it has been changed from $20cm$ to $200cm$. The LDV stays at the same position, but the ADV is moved at all the different downstream positions. The velocimeters are always at the centre of the tank section and the flow velocity stays $U_\infty = 0.8m/s$ with the same turbulence intensity.

The first presented result is the maximum of the cross-correlation ρ, for both components u and w, versus the velocimeter distance d (figure 13). As observed on this figure, these coefficients decrease when the distance increases from values higher than 0.8 for $d < 50cm$ to values lower than 0.6 at $200cm$.
The time-lag τ where the maximum of the cross-correlation is observed varies linearly with the distance d as depicted on figure 14 and as expected. According to this figure, it requires $2.5s$ for the flow to travel from LDV to ADV spaced by $2m$, which is in agreement with the averaged flow velocity of $0.8m/s$. A slight difference is however noticeable between the two components of the velocity and τ_{uu} is lower than τ_{ww}, especially for the highest distances d. As explained in the previous subsection, the high-frequency noise observed on u for the ADV is the reason why $\rho_{uu} < \rho_{ww}$ and may explain the slight difference on the time-lag τ.

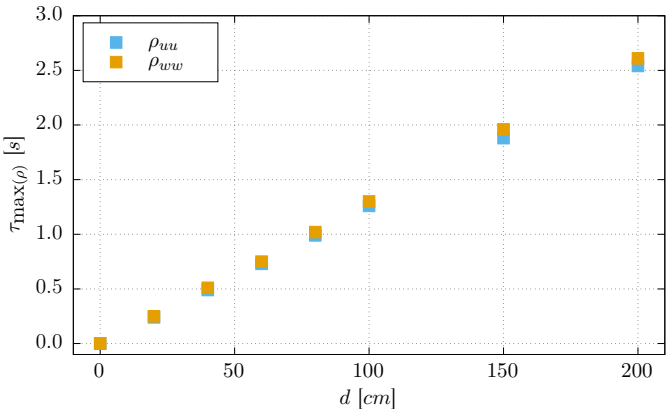

Figure 14: Time-lag τ corresponding to the maximum value of the cross-correlation ρ

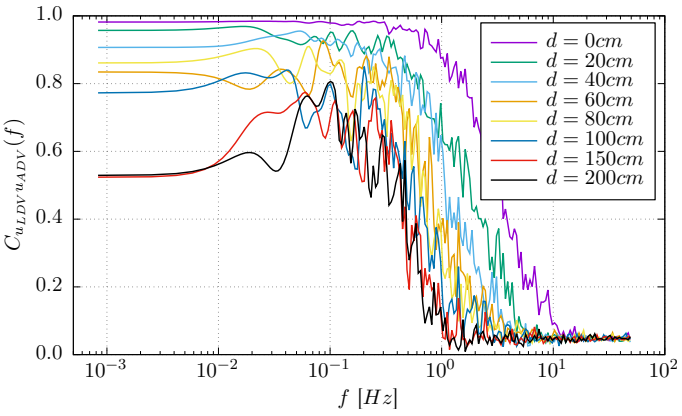

Figure 15: Coherence function $C_{u_{LDV}u_{ADV}}$ for all the tested distances

The coherence functions for u and w are processed and plotted on figures 15 and 16 respectively. These curves are interesting for different aspects. Firstly, the amplitudes of these coherence function decrease when the distance increases: from values very close

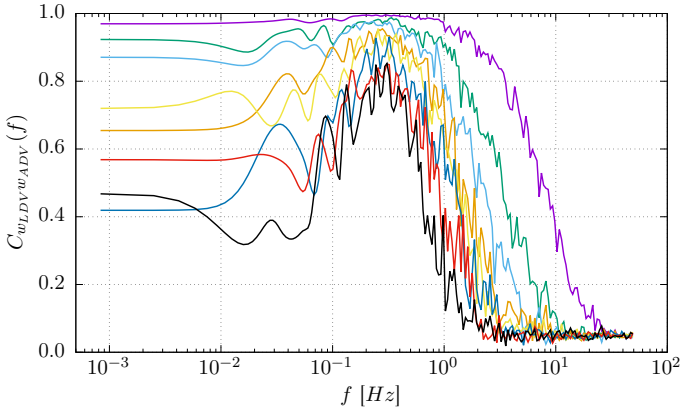

Figure 16: Coherence function $C_{w_{LDV}w_{ADV}}$ for all the tested distances

to 1 on a large range of frequencies when $d = 0$, only the maximum value stays close to 0.8 on a narrow band of frequencies for $d \geq 150cm$. Secondly, a strong decrease of the coherence is observed for the lowest frequencies, which are lower than 0.6 as soon as $d \geq 100cm$ for w and $d \geq 150cm$ for u. Finally, the maximum frequency for which the coherence stays valid ($C(f) > 0.6$) decreases quickly when the distance d increases (figure 17).

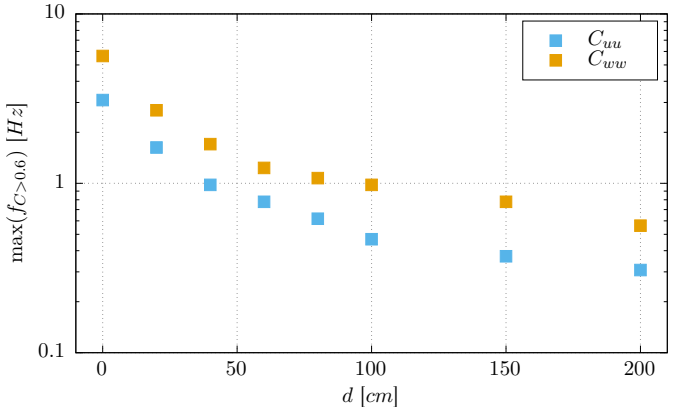

Figure 17: Maximum frequency for which C_{uu} and C_{ww} is higher than 0.6

From values $f = 3Hz$ and $f = 6Hz$ observed for $d = 0$ for u and w respectively, the maximum frequencies fall to $f = 0.5Hz$ and $f = 1Hz$ for $d = 1m$ and $f = 0.3Hz$ and $f = 0.6Hz$ for $d = 2m$. For the two highest distances ($d \geq 150cm$) the coherence function stays only valid on a short band of frequencies.

The distance between the measurement points has a strong effect on all the parameters observed in this section. Mainly because of the turbulence intensity, the flow velocity characteristics differ from one point to another: when the distance between the velocimeters increases, the velocity characteristics change along this distance that makes the correlation more difficult to process.

5 CONCLUSION

As noticed in this study, an upstream velocity measurement is required to improve the accuracy of the performance characterization of a marine turbine. This flow measurement has to be performed simultaneously and synchronously with the turbine parameters. It is necessary to keep in mind that the difference in term of measurement size between two velocimeters, as well as between a velocimeter and a turbine area, can cause a loss in the coherence of the signals, particularly for the high frequencies. The smallest turbulent structures in the flow, with the highest frequencies, are not seen in the same way by two different devices with two different sizes: the smallest size enables to perceive the smallest structures. In addition, the distance between the flow measurement and the turbine can increase the loss of information between the upstream velocity signal and the turbine parameters. On the other hand, the momentum theory shows that the flow speed should reduce from free-stream conditions far upstream of the turbine to the velocity incident at the rotor plane. In order to better understand this last point, additional measurements have to be performed to take into account the competing requirements between an upstream undisturbed flow speed and a measurement that is correlated with the flow incident on the turbine.

The turbulence characteristics in term of iso or anisotropy, energy level and spatial repartition, effect on turbine performances must be also addressed. Indeed, (Ikhennicheu et al. 2017) highlight that a particular attention should be paid in presence of large velocity fluctuations, with high turbulence rate, coming from bathymetry variations. These low frequency structures, with a diameter up to the diameter of the turbine, affects the efficiency of the turbine and the fatigue of the blades. To assess these points, the performances of the turbine, in term of the classical power and thrust coefficients, should be processed. The blades bending moment coefficients should be analysed as well, in a temporal and spectral point of view. A good spatial flow measurements, like obtained with PIV measurements for the upstream flow characterization, should then be preferred.

6 ACKNOWLEDGEMENTS

This work received the support of the MET-CERTIFIED project, funding from the Interreg 2 Seas programme 2014-2020, co-funded by the European Regional Development Fund under subsidy contract N. 2S01-020.

REFERENCES

Dantec Dynamics (2018). Laser Doppler Anemometry Measurement Principles.

Day, S., I. Penesis, A. Babarit, A. Fontaine, Y. He, M. Kraskowski, M. Murai, F. Salvatore, & H. Shin (2014). ITTC Recommended Guidelines: Model tests for current turbines (7.5-02-07-03.9). In *Proceedings of the 27th International Towing Tank Conference (Recommended Procedures and Guidelines register)*, Copenhagen, Denmark, pp. 1–17.

Specialist Committee on Testing of Marine Renewable Device.

Durán Medina, O., F. G. Schmitt, R. Calif, G. Germain, & B. Gaurier (2017). Turbulence analysis and multiscale correlations between synchronized flow velocity and marine turbine power production. *Renewable Energy 112*, 314 – 327.

Gaurier, B., G. Germain, & J.-V. Facq (2017). Experimental study of the Marine Current Turbine behaviour submitted to macro-particle impacts. In *Proceedings of the 12th European Wave and Tidal Energy Conference*, Cork, Ireland.

Gaurier, B., G. Germain, J.-V. Facq, C. Johnstone, A. Grant, A. Day, E. Nixon, F. Di Felice, & M. Costanzo (2015). Tidal energy "Round Robin" tests comparisons between towing tank and circulating tank results. *International Journal of Marine Energy 12*, 87 – 109. Special Issue on Marine Renewables Infrastructure Network.

Germain, G., A. Chapeleau, B. Gaurier, L.-M. Macadre, & P. Scheijground (2017). Testing of marine energy technologies against international standards. Where do we stand? In *Proceedings of the 12th European Wave and Tidal Energy Conference*, Cork, Ireland.

Germain, G., B. Gaurier, M. Harrold, M. Ikhennicheu, P. Scheijgrond, A. Southall, & M. Träsch (2018). Protocols for testing marine current energy converters in controlled conditions. Where are we in 2018? In *Proceedings of the 4th Asian Wave and Tidal Energy Conference*, Taipei, Taiwan.

Ikhennicheu, M., P. Druault, B. Gaurier, & G. Germain (2017). Experimental tidal power site bathymetry representation for turbulence characterization. In *Proceedings of the 12th European Wave and Tidal Energy Conference*, Cork, Ireland.

Ingram, D., G. Smith, C. Bittencourt-Ferreira, & H. Smith (2011). *Protocols for the Equitable Assessment of Marine Energy Converters* (1st ed.). Edinburgh, UK: The Institute for Energy Systems.

Marine Energy (2013). Wave, tidal and other water current converters - Part 200: Electricity producing tidal energy converters - Power performance assessment. Technical Report 27.140, International Electrotechnical Commission.

Marine Energy (2015). Wave, tidal and other water current converters - Part 201: Tidal energy resource assessment and characterization. Technical Report 27.140, International Electrotechnical Commission.

Marine Energy (2019). Wave, tidal and other water current converters - Part 202: Scale testing of tidal stream energy systems. Technical report, International Electrotechnical Commission.

McNaughton, J., S. Harper, R. Sinclair, & B. Sellar (2015). Measuring and modelling the power curve of a commercial-scale tidal turbine. In *Proceedings of the 11th European Wave and Tidal Energy Conference*, Nantes, France.

Mycek, P., B. Gaurier, G. Germain, G. Pinon, & E. Rivoalen (2014). Experimental study of the turbulence intensity effects on marine current turbines behaviour. Part I: One single turbine. *Renewable Energy 66*, 729 – 746.

Nortek USA (2018). Vectrino.

Payne, G. S., T. Stallard, & R. Martinez (2017). Design and manufacture of a bed supported tidal turbine model for blade and shaft load measurement in turbulent flow and waves. *Renewable Energy 107*, 312 – 326.

Sixaxes (2017). Société française, spécialisée dans l'étude et la fabrication de chaîne de mesure de force depuis plus de 22 ans.

Thomson, J., B. Polagye, V. Durgesh, & M. C. Richmond (2012). Measurements of turbulence at two tidal energy sites in puget sound, WA. *IEEE Journal of Oceanic Engineering 37*(3), 363–374.